12-1-1973

# Size distribution analysis of polydisperse, monodisperse, and chemically mixed polymer latex systems via a combination of light scattering and ultracentrifugation techniques

Robert Cembrola

# SIZE DISTRIBUTION ANALYSIS OF POLYDISPERSE, MONODISPERSE, AND CHEMICALLY MIXED POLYMER LATEX SYSTEMS VIA A COMBINATION OF LIGHT SCATTERING AND ULTRACENTRIFUGATION TECHNIQUES

ROBERT J. CEMBROLA

DECEMBER, 1973

THESIS

SUBMITTED IN PARTIAL FULFILLMENT OF THE

REQUIREMENTS FOR THE DEGREE OF MASTER OF SCIENCE

APPROVED:

Thomas P. Wallace
Project Advisor

Robert E. Gilman
Department Head

Names Illegible
Library

Rochester Institute of Technology
Rochester, New York
Department of Chemistry

TABLE OF CONTENTS

TABLES

FIGURES

DEDICATION

To my parents

ACKNOWLEDGMENT

I would like to thank Dr. Thomas P. Wallace for his guidance and understanding, it was deeply appreciated.

Also to Mrs. Sharon Valyear who typed the manuscript.

## ABSTRACT

The use of angular light scattering techniques has proved to be of the highest precision for the size distribution analysis of colloidal size spheres, but is inherently limited to quite narrow, monomodal size distributions of particles of a single chemical component. These limitations can be overcome to a limited degree by a technique that utilizes light scattering and a preparative ultracentrifuge. The latter fractionates the colloidal particles according to density (i.e., chemical composition) and/or size. Applying the zonal ultracentrifugation technique, both types of separation take place in the presence of a density gradient and ultimately fractionated samples are obtained which are then characterized by light scattering to provide size distribution parameters. The size parameters assigned to each fraction can then be used to reconstruct the original size distribution.

A further use of the technique will be demonstrated using a %T vs. fraction number curve obtained from a recording spectrophotometer which is on line between the rotor and the fraction collector. By calibration of the rotor using the ultracentrifuge-light scattering technique above, the %T vs. fraction number curve can be converted to a plot of relative frequency vs. diameter.

The above techniques will be applied to broad continuous distributions, monomodal distributions and to a mixture of polystyrene, polyvinylchloride, and polyvinylacetate latexes of different sizes.

# BACKGROUND

A method for determining the density of small quantities of solutions using a density gradient was introduced in 1937 by Linderstrom-Lang.[1] In 1938, Behrens utilized density gradient centrifugation to separate particles according to density in systems with little solvent-solute interaction, such as biological cells suspended in a gradient of organic solvents.[2] Density gradient centrifugation as presently used was conceived and developed by M.K. Brakke.[3] Brakke realized the inherent advantages of zonal separation procedures and conceived the idea of using a density gradient in which the particles form an isopycnic band at equilibrium.

The availability of the Spinco preparative ultracentrifuge and the introduction of suitable scanning systems led to a rapid spread in use of the technique during the 1960's. Numerous variations of the method have been developed. For example, it has been used for purification, assay, measuring sedimentation rates, densities, molecular weights, and correlating biological and chemical activity with sedimentation rate or density.[4]

Anderson and associates developed the zonal rotor centrifuge during the 1960's and demonstrated some of its applications in biochemical systems.[4]

The rotor in a zonal centrifuge is a hollow compartment of varying shape and capacity divided by vertical septa into sector shaped compartments. Two fluid handling lines run through an upper shaft and

connect the edge of the rotor with the central core by a flat rotating seal which presses against an external static seal. All operations, including introduction of the density gradient and the sample layer, and recovery of the gradient with its separated zones of particles, are carried out with the rotor spinning.

Particles in a medium less dense than themselves will sediment through that medium when a centrifugal force is applied. The velocity v at which spherical particles sediment is described by Stokes Law,[4]

$$V = \frac{2}{9} q r^2 \frac{(\rho_P - \rho_M)}{\eta}$$

where $\rho_P$ and $\rho_M$ are the density of the particle and the medium respectively, $r$ the radius of the particle, $q$ the applied centrifugal force, and $\eta$ the viscosity of the medium.

The many variations of density gradient centrifugation fall into two classes. First, a separation is based on a density difference. The upper boundary of the gradient should be of a greater density than that of any of the particles. The particles will sediment until they reach their own density and form an isopycnic band in the rotor. This technique is termed zonal equilibrium centrifugation. Second, a separation is based on different sedimentation rates due to different size and shape. Larger particles will sediment at a faster rate and will spread out through the gradient. In this case, the upper density must be below that of the particles otherwise they will accumulate at the point where $\rho_P = \rho_M$. During pump-out the force

is not strong enough to cause further sedimentation and the gradient maintains the separation. This technique is termed rate zonal centrifugation. The following is a brief outline of a typical zonal centrifugation:

Preparation of Rotor

While the empty rotor is spinning at 2000-3000 rpm, the seal assembly is placed on the spinning rotor head. A continuous flow pump establishes a density gradient which is pumped into the rotor with the lowest density at the center and the highest density at the outer edge. A programmed cam is used to provide the desired gradient.

Introduction of Sample

The sample is slowly introduced into the center of the rotor with a syringe to maintain a narrow sample band that will not disturb the gradient. This process displaces an equal volume from the outer edge, and care must be taken to avoid getting air into the rotor. Once the sample is in the rotor it is capped, the chamber is closed, and a vacuum is established. The rotor speed is then increased, and at the higher speed the particles begin to move away from the center of rotor with the larger and more dense particles moving at a faster rate than the smaller and less dense ones. As this process continues the particles separate in the rotor according to size and density. Once a particle reaches its own density its outward movement ceases. In a velocity run, when the rotor speed is reduced to 2000-3000 rpm, the particles become suspended in the gradient as the force is insufficient to cause further appreciable motion (sedimentation or diffusion).

Pump-Out

With the rotor set at 2000-3000 rpm the chamber is opened, the cap removed, and the seal assembly is again placed on the rotor. The pump-out can proceed in either of two ways. A concentrated solution of the same species as that of the gradient can be pumped into the outer edge and displace the gradient at the center. In the other method, water is pumped into the center and forces the gradient out the edge. These processes continue until the entire gradient is displaced. The displaced gradient is usually channeled into a flow through cell of a spectrophotometer and then into a fraction collector. The spectrophotometer can be used to determine the position of the particles in the rotor, the nature of the size distribution, and which fractions are to be analyzed. These fractions are then analyzed by a light scattering technique developed for spherical particles.

Light Scattering

The form of the angular scattering pattern from an isotropic spherical particle is dependent on the relative refractive index m (i.e., the ratio of the refractive index of the sphere to the medium in which it is immersed), the optical size $\alpha = \frac{\pi D}{\lambda}$, where D is the particle diameter and $\lambda$ the wavelength of light in the medium.[5] The Mie angular intensity function $(i_1)_\theta$ for the vertically polarized component of scattered light from a scattering system of finite polydispersity is given by[6]

where $(i_1')_\theta$ is the Mie intensity function at angle $\theta$ for a single sphere of optical size $\alpha$, and $p(\alpha)$ is the frequency function for the zeroth-order logarithmic distribution.[7] Therefore $p(\alpha)d\alpha$ gives the fraction of particles with sizes between $\alpha$ and $\alpha + d\alpha$. A similar expression exists for the horizontally polarized component of scattered light $(i_2)_\theta$. This distribution function has a slight positive skew and is expressed as

$$p(\alpha) = K \exp\left\{-(\ln\alpha - \ln\alpha_m)^2/2\sigma_o^2\right\} \quad [5]$$

where $K$ is a normalization constant, $\alpha_m$ is the modal optical size, and $\sigma_o$ is a distribution width parameter (i.e., polydispersity) which is related to the standard deviation by

$$\sigma = \alpha_m \sigma_o \left\{1 + \frac{7\sigma_o^2}{2!} + \frac{37\sigma_o^4}{3!} + \cdots\right\} \quad [5]$$

The polarization ratio $\rho_\theta$ is defined as $\frac{(i_2)_\theta}{(i_1)_\theta} = \frac{H_{h,\theta}}{V_{v,\theta}}$ where $H_{h,\theta}$ is the Rayleigh ratio for the horizontally polarized component of the radiant scattered intensity per unit solid angle from an incident horizontally (subscript $h$) polarized beam of unit irradiance; the definition of $V_{v,\theta}$ follows that of $H_{h,\theta}$.[5]

Mie angular intensity functions $i_1, i_2$, as well as the polarization ratio $\rho_\theta$ have been calculated for various sets of size distribution parameters $(\alpha, \sigma_o, m)$. A computer program was obtained from Clarkson

College of Technology which compares the theoretical and experimental scattering patterns to give a best fit in the form of an error contour map.[8] The fit from the contour map provides size distribution parameters $\alpha_M$ and $\sigma_0$ .

The spectrophotometer records absorbance at a specific wavelength for each fraction collected. This absorbance can be converted through a series of relationships to give the number of particles per $cm^3$ being observed. First, absorbance is converted to turbidity $\tau$ by

$$\tau = \frac{2.303\,A}{\ell}$$

where $A$ is absorbance and $\ell$ is the path length of the cell. A scattering cross-sectional coefficient $Q$ , which is dependent on optical size $\alpha_M$ and the wavelength of light used, is next obtained from a table.[6] This coefficient is then used to obtain a term

$$R = \pi r^2 Q$$

where $r$ is the radius of the particle. The number of particles is then obtained through the relationship $N = \frac{\tau}{R}$

The output from the spectrophotometer can then be converted to a number of particles versus fraction number which is the ultimate objective of the technique.

# EXPERIMENTAL

## Instrumentation

Beckman L2-65B Ultracentrifuge, Beckman DB-G Grating Spectrophotometer, Beckman Fraction Collector Model 132, Bausch and Lomb Refractometer, Beckman Model 141 Gradient Pump, B-15 Aluminum Rotor, Beckman $w^2t$ Integrator, Sofica Light Scattering Photometer.

## Continuous Distribution System

A continuous distribution of polystyrene latex particles was prepared from ten "monodisperse" Dow samples 1053-14-1 through 1053-14-10. These were characterized by light scattering and had a size range from 400 to 670 nm. The mixture was diluted with distilled water to a percent solids concentration of 0.1-1.0%.

The object of the experiment was to fractionate the system according to size and obtain fractions of narrow size distribution. A series of experiments were run to determine the optimum conditions to achieve those objectives.

In all of the separation runs, the following conditions were always maintained. The gradients were prepared using sucrose solutions and were introduced into the rotor at a rate of 29 ml/min by a programmed cam attached to the pump, which produced a linear output gradient. The sample size was 40 ml with no overlay solution. An overlay solution, usually water, is sometimes added after the sample to push it into the gradient to insure sedimentation. The rotor was accelerated to 15,000 rpm for varying lengths of time. During pump-

out the rate was 17 ml/min for both techniques. The volume of the fractions collected was 8.0 ml. Since the total volume of the B-15 rotor is 1665 ml, the number of fractions obtained from a displaced gradient is 208.

The two variables to be determined were the range of the gradient, and the total force on the particles required to "string out" the particles according to size. (When too large a force is applied the string will begin to collapse upon itself. This has been termed an accordian effect and must be avoided.) Optimum separation will be obtained when the string is stretched to its maximum before contracting.

Initially a gradient was selected, and the optimum force found by trial and error. The width of the gradient determines the resolution of the separation. For the continuous distribution the wider the gradient the better the resolution. The upper end of the gradient must not exceed the density of the particles. Polystyrene has a density of 1.054 gm/cc, which corresponds to 13.3% sucrose. During a separation the sample should be contained within the inner 75% volume capacity of the rotor. Proceeding from the center, the change in concentration per unit length, dc/dr, becomes very small, thereby reducing the stabilizing effect of the gradient.

The first successful gradient was 11.0-13.2% sucrose, however, the $\sigma$ (i.e., polydispersity) values were higher than those of the original samples. Since the upper end of the gradient was close to the density of the particles it was decided to lower the high end to a 10% sucrose solution, with a corresponding decrease of the lower end. A series of experiments were then run using 10% sucrose as the upper limit and varying the lower limit.

For a given set of conditions the rotor was calibrated to give a particle size for a specific fraction number. Individual samples were then run under those same conditions to determine the reproducibility of the experiment.

In all the above experiments the center pump-out technique was employed, therefore, a separation was next attempted using the edge-unloading method. The separation may be improved by this technique because there is no reversal of flow which could cause remixing. The gradient used was 3.0-10.0% and the force was approximately the same as that for the center unloading technique. This force, however, was too great as the particles had traversed the entire rotor and were being observed in the first fractions. This piling up at the rotor wall produced $\sigma$ values which were larger than from the center pump-out results. In our next run the length was reduced to keep the latex particles from reaching the rotor wall, most of the particles, however, did not obtain a sufficient applied force to move into the gradient and were not pumped-out. Meanwhile a small fraction of large particles did sediment to the rotor wall.

There appears to be a critical force that must be applied on the particles in order to initiate sedimentation and this force is dependent on particle size and density. The size distribution combined with a limited rotor volume prevents a full extension of the sample for fractionation.

Single Monodisperse Sample

Having demonstrated the ability to fractionate latex particles according to size, a single Dow sample was fractionated to determine the extent that a size distribution can be narrowed. Dow polystyrene

latex 1053-14-6, characterized by light scattering to have a $D_m$ = 564 nm. and $\sigma$ = 40 nm., was used as the sample. The same experimental procedures applied to the continuous distribution apply here.

The initial run used a 5.0-10.0% sucrose gradient with the center unloading technique. An applied force similar to that used for the continuous distribution was employed. The gradient was then narrowed to 8.0-10.0% sucrose to see its effect on $\sigma$. For both of these gradients, runs were made in duplicate.

It was felt that the edge-unloading method could be applied to this system because of the narrow size distribution and was tested next. An 8.0-10.0% sucrose gradient was used, and run in duplicate.

The next step in all the above experiments was to use fractions that had lower $\sigma$ values and refractionate them. A number of adjacent fractions were combined and diluted to a concentration just below the lower end of the sucrose gradient. For the separation an 8.0-10.0% gradient was used with the edge-unloading method.

Chemically Mixed Latex System

A mixed latex system was prepared using Dow polystyrene 1053-14-1 ($D_m$ = 409 nm., $\sigma$ = 20 nm.), Monsanto polyvinyl chloride 540876 ($D_m$ = 419 nm., $\sigma$ = 25 nm.), and Kodak polyvinyl acetate ($D_m$ = 228 nm., $\sigma$ = 30 nm.) The above three polymer latexes will be symbolyzed as PS, PVC, and PVA respectively.

The first attempt at preparing the mixture resulted in a coagulation of the particles. In the literature this phenomena was discussed and methods were suggested to both cause and prevent precipatation.[9] It appears that there is a concentration dependence for

coagulation, and below a critical level no coagulation occurs. This concentration restriction limited the analysis of the fractions and will be discussed in more detail below.

The original experiment planned an equilibrium run to separate the chemical species by density, followed by a velocity run to separate the individual components by size. The first attempt was an equilibrium separation on just a PS-PVC mixture with an 8.0-50.0% sucrose gradient using the center unloading technique. The polystyrene came out as a narrow band at 13.3% sucrose, while no peak was observed for the PVC despite additional pump-out. The conclusion was that the density of the PVC latex exceeds the sucrose solution and continues sedimenting at a rate faster than that of pump-out. A velocity zonal separation, changing only the applied force to obtain the particles before they reached the edge, was successful. However, the entire PVC sample could not be recovered due to continued sedimentation. The high density of PVC and also of PVA latex necessitated the use of the edge-unloading method. The continuity of flow along with different sedimentation rates should produce a separation, where the particle with the larger sedimentation rate will leave the rotor first.

A short velocity run using a 10.0-50.0% sucrose gradient was used on the mixture of PS, PVC, and PVA. Light scattering analysis was used to determine chemical composition and purity.

Another mixture of the three latexes was also prepared for separation. This consisted of Dow PS 1053-14-7 ($D_m$ = 585 nm., $\sigma$ = 40 nm.), Monsanto PVC 540876, ($D_m$ 419 nm., $\sigma$ = 25 nm.), and

Kodak PVA ($D_m$ 228 nm., $\sigma$ = 30 nm.). The reason this new mixture was run was the similarity of size between the PVC and PS latex samples in the former mixture.

Sample Code Used in Tables

It is a three letter, three number code referring to the run.

1. First letter refers to the sample (C - continuous, S - single and M - mixed).
2. Second letter refers to frequency of fractionation (F - first fractionation, R - second fractionation).
3. Third letter refers to unloading technique (C - center unloading, E - edge-unloading).
4. First number is lower end of gradient.
5. Second number is upper end of gradient.
6. Third number refers to frequency of the run.

## RESULTS AND DISCUSSION

### Continuous Distribution System

The ten Dow polystyrene latex samples were characterized separately by the light scattering technique discussed below. Frequency versus diameter plots were generated for each sample to insure that there was a continuous distribution.

TABLE 1

Average Size and Size Distribution of Dow Polystyrene Latex Samples Determined from Light Scattering Analysis

| Dow Sample | $D_m$ (nm.) ± 5 nm. | $\sigma$ (nm.) ± 5 nm. |
|---|---|---|
| 1053-14-1 | 409 | 20 |
| 1053-14-2 | 435 | 30 |
| 1053-14-3 | 460 | 40 |
| 1053-14-4 | 502 | 35 |
| 1053-14-5 | 538 | 25 |
| 1053-14-6 | 564 | 40 |
| 1053-14-7 | 585 | 40 |
| 1053-14-8 | 626 | 35 |
| 1053-14-9 | 657 | 45 |
| 1053-14-10 | 678 | 45 |

An initial gradient of 11.0-13.2% sucrose was decided upon, with the upper limit just below the density of the latex particle. The center pump-out technique was used with a 30% sucrose displacing solution. Latex began to emerge from the rotor at fraction 40 and was spread out over 70 tubes. The $\omega^2 t$ integrator read 940 x $10^7$ $rad^2/sec$.

Figure 1. Frequency vs. Diameter Plot of the 10 Dow Polystyrene Latex Samples

Fig. 1

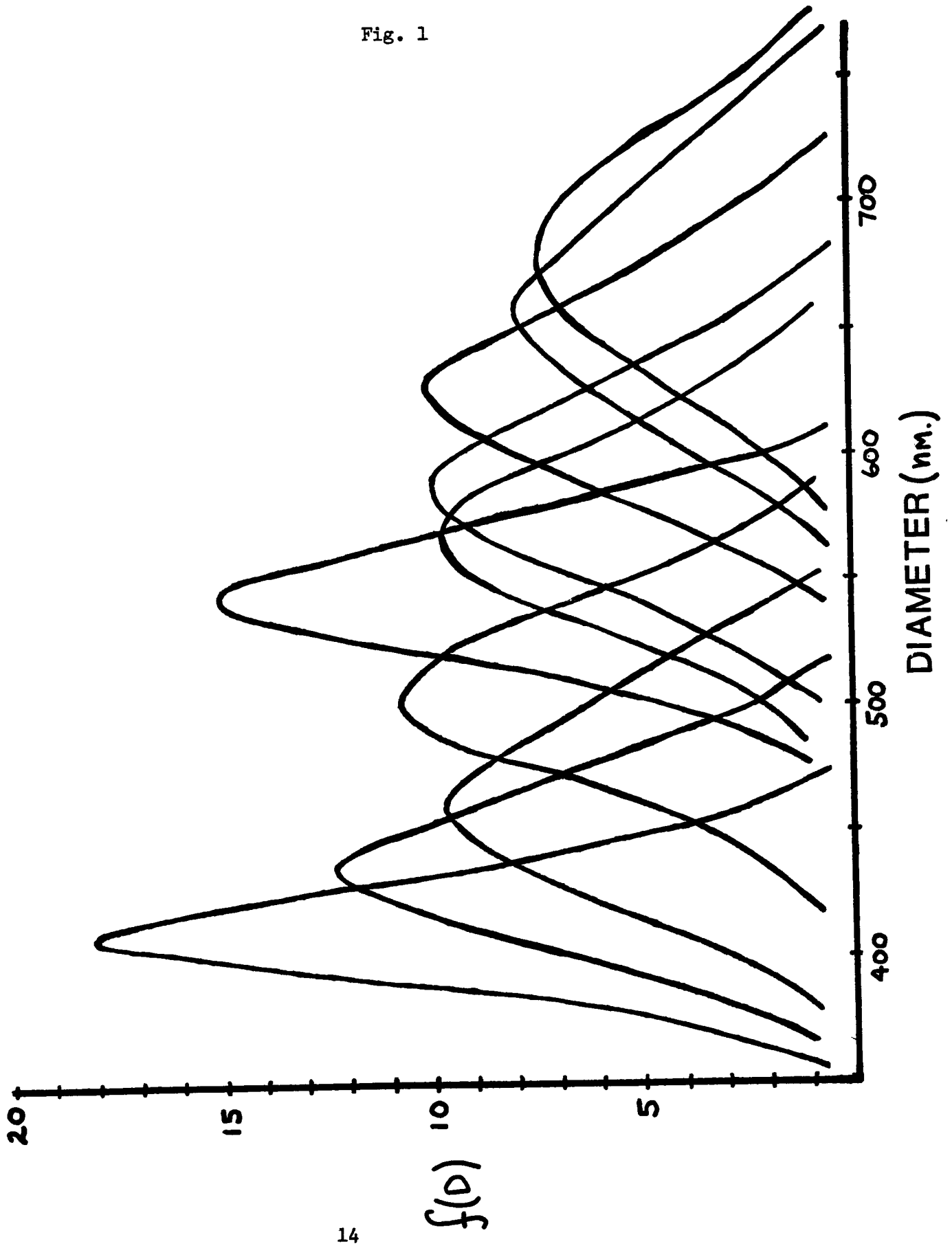

when half the latex was recovered. In reporting all $\omega^2 t$ readings the preceeding criteria was observed. A total of 11 fractions were analyzed for particle size and size distribution by light scattering. The fractions were also analyzed for % sucrose with a differential refractometer. Plots of particle size versus fraction number and % sucrose verus fraction number were compared to note any correlation. The plot of particle size versus fraction number is linear, corresponding with the linear portion of the % sucrose versus fraction number graph. The $\sigma$ values were slightly higher than those of the initial components.

A separation was next performed using an 11.3-13.2% sucrose gradient under similar conditions. The applied force was $980 \times 10^7$ $rad^2/sec.$, and the latex initially appeared at fraction 30 and spread out over 60 fractions. A total of 9 fractions were analyzed and the $\sigma$ values had a wider range than the previous run.

Anderson noted[4] that the distribution of sizes (sedimentation coefficients) dictated the optimum gradient. For a large distribution a wide gradient should be used. To observe the effect of the gradient width on the resolution, a series of experiments were run on the continuous distribution. The upper end of the gradient was lowered to 10.0% sucrose to increase the effective volume of the rotor. The upper end of the 13.2% sucrose maximum gradient was close to the density of the particles so that their velocities approached zero as they neared the rotor wall. The resultant slowdown could cause remixing and was the reason the upper limit of the gradient was lowered to 10% sucrose.

A summary of results is listed in Table 4. The standard deviation ( $\sigma$ ) appears to be dependent on the applied force to a greater extent

TABLE 2

Light Scattering Results of Fractions from Run CFC 11.0-13.2-1

Run: CFC - 11-13.2-1 $\omega^2 t = 940 \times 10^7$ rad.$^2$/sec.

Sample Range: Fraction 40-110

| Fraction Number | $D_m$ (nm.) ± 10 nm. | $\sigma$ (nm.) ± 5 nm. |
|---|---|---|
| 45 | 388 | 40 |
| 50 | 398 | 50 |
| 55 | 435 | 45 |
| 60 | 450 | 50 |
| 65 | 481 | 55 |
| 70 | 512 | 45 |
| 75 | 528 | 55 |
| 80 | 548 | 55 |
| 85 | 574 | 55 |
| 90 | 595 | 55 |
| 95 | 621 | 55 |

Figure 2. Percent Sucrose vs. Fraction Number Plot of Run CFC 11.0-13.2-1

Fig. 2

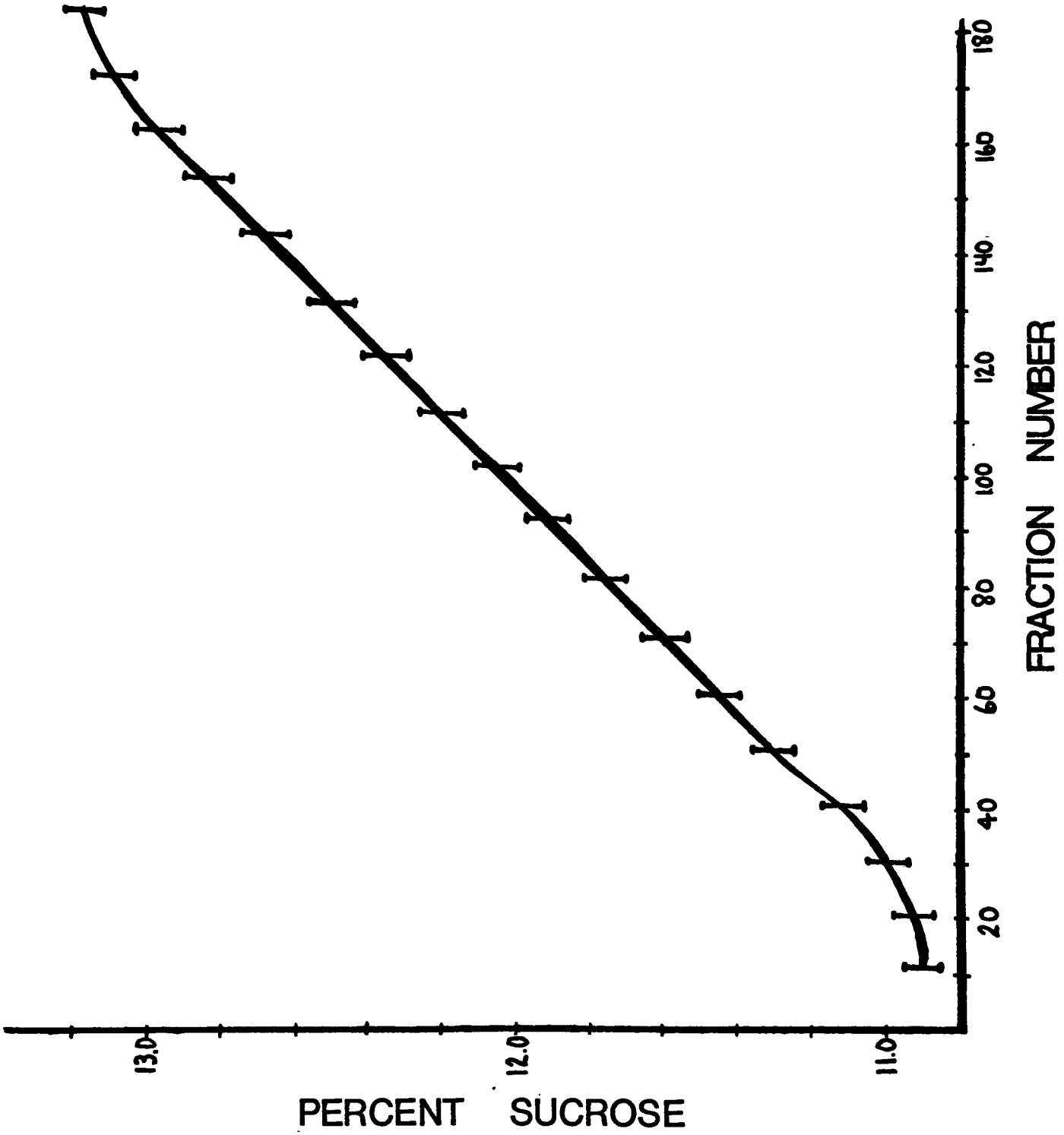
13.0
12.0
11.0
PERCENT SUCROSE
20
40
60
80
100
120
140
160
180
FRACTION NUMBER

Figure 3. Particle Size vs. Fraction Number Plot of Run CFC 11.0-13.2-1

Fig. 3

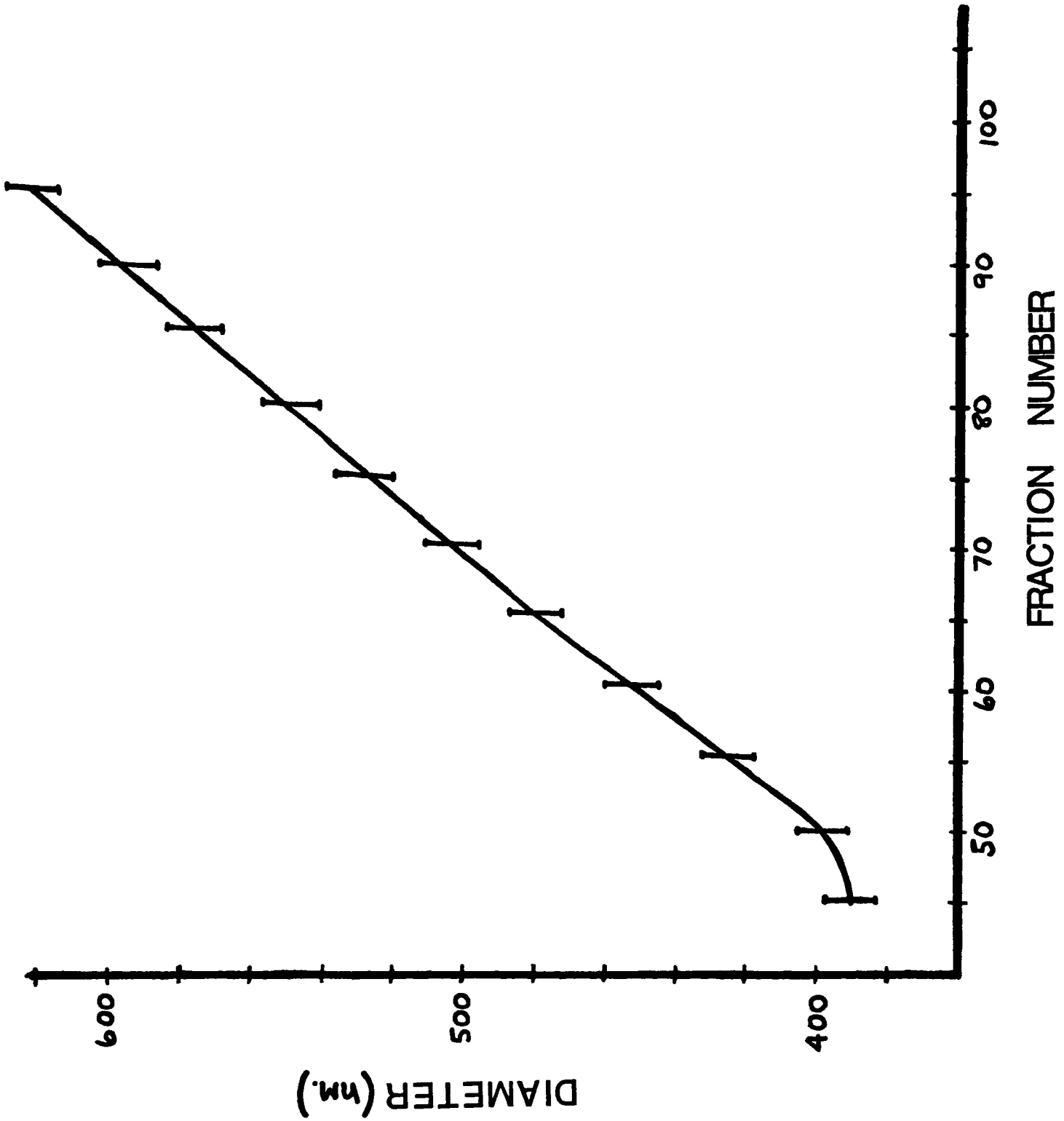

TABLE 3

Light Scattering Results of Fractions from Run CFC 11.3-13.2-1

Run: CFC - 11.3-13.2-1 $\omega^2 t = 980 \times 10^7$ rad.$^2$/sec.

Sample Range: Fraction 30-90

| Fraction Number | $D_m$ (nm.) ± 10 nm. | $\sigma$ (nm.) ± 10 nm. |
|---|---|---|
| 35 | 414 | 25 |
| 40 | 429 | 35 |
| 45 | 445 | 50 |
| 50 | 476 | 70 |
| 55 | 507 | 70 |
| 60 | 559 | 70 |
| 65 | 595 | 65 |
| 70 | 611 | 70 |
| 75 | 626 | 65 |

than the width of the gradient. In each case when a particular gradient was run at a lower $\omega^2 t$ the $\sigma$ values were significantly lower, while a comparison of each gradient showed a slight downward trend in $\sigma$ as the gradient width increased. These two factors can be combined into a single variable by a modification of Stokes Law;

$$\omega^2 t \times (\rho_p - \rho_o)$$

where $\rho_p$ is the density of the particle and $\rho_o$ is the density of the medium at the lower end of the sucrose gradient. This variable provides a gauge for further studies on polydisperse systems by establishing a narrow range of values for a successful separation. A successful separation is obtaining a unique fit of theoretical and experimental light scattering data. The smaller the standard deviation of the fraction the better the separation. The best fits were obtained when the product of $\omega^2 t \times (\rho_p - \rho_o)$ was 6.0 $\pm$ 0.25. The system was not tested below an $\omega^2 t \times (\rho_p - \rho_o)$ value of 5.75 since the force necessary to cause sedimentation required a threshold $\omega^2 t$ value.

The next objective was to calibrate the rotor for particle size analysis using run CFC 3-10-2 as the model. A plot of particle size versus fraction number was fitted by a least squares program to obtain the calibration curve. The equation for the line is

Diameter (nm.) = 3.17 (Fraction Number) + 351.

The above equation obtained from the data resulted in a standard deviation for the slope and intercept of 0.37 and 9.5 respectively, with a correlation coefficient of .991. With the calibration curve established, various single latex samples were run under similar

TABLE 4

Results of Light Scattering Analysis for a Series of Runs on the Continuous Distribution System

Run: CFC 8-10-1 $\omega^2 t = 258 \times 10^7$ rad.$^2$/sec.

Sample Range: Fraction 7-140 $\omega^2 t \times (\rho_p - \rho_o) = 5.75$

| Fraction Number | $D_m$ (nm.) ± 10 nm. | $\sigma$ (nm.) ± 10 nm. |
|---|---|---|
| 20 | 414 | 30 |
| 30 | 424 | 40 |
| 40 | 445 | 55 |
| 50 | 492 | 60 |
| 60 | 533 | 60 |
| 70 | 574 | 60 |
| 80 | 611 | 50 |

Run: CFC 7-10-1 $\omega^2 t = 274 \times 10^7$ rad.$^2$/sec.

Sample Range: Fraction 10-170 $\omega^2 t \times (\rho_p - \rho_o) = 7.21$

| Fraction Number | $D_m$ (nm.) ± 10 nm. | $\sigma$ (nm.) ± 10 nm. |
|---|---|---|
| 30 | 419 | 30 |
| 40 | 440 | 45 |
| 50 | 471 | 50 |
| 60 | 502 | 55 |
| 70 | 523 | 55 |
| 80 | 543 | 60 |
| 90 | 564 | 60 |
| 120 | 621 | 55 |
| 155 | 621 | 70 |

Run: CFC 7-10-2 $\omega^2 t = 230 \times 10^7$ rad.$^2$/sec.

Sample Range: Fraction 10-150 $\omega^2 t \times (\rho_p - \rho_0) = 6.05$

| Fraction Number | $D_m$ (nm.) ± 5 nm. | $\sigma$ (nm.) ± 5 nm. |
|---|---|---|
| 20 | 414 | 25 |
| 30 | 419 | 35 |
| 40 | 471 | 50 |
| 50 | 507 | 45 |
| 60 | 533 | 50 |
| 70 | 564 | 55 |
| 80 | 600 | 55 |
| 90 | 616 | 55 |
| 100 | 631 | 50 |

Run: CFC 6-10-1 $\omega^2 t = 191 \times 10^7$ rad.$^2$/sec.

Sample Range: Fraction 10-140 $\omega^2 t \times (\rho_p - \rho_0) = 5.75$

| Fraction Number | $D_m$ (nm.) ± 10 nm. | $\sigma$ (nm.) ± 5 nm. |
|---|---|---|
| 20 | 409 | 25 |
| 30 | 414 | 30 |
| 40 | 430 | 45 |
| 50 | 450 | 65 |
| 60 | 486 | 70 |
| 70 | 548 | 55 |
| 90 | 590 | 55 |

Run: CFC 5-10-1 $\omega^2 t = 210 \times 10^7$ rad.$^2$/sec.

Sample Range: Fraction 5-145 $\omega^2 t \times (\rho_p - \rho_0) = 7.22$

| Fraction Number | $D_m$ (nm.) ± 10 nm. | $\sigma$ (nm.) ± 10 nm. |
|---|---|---|
| 30 | 414 | 30 |
| 40 | 419 | 35 |
| 50 | 429 | 50 |
| 70 | 476 | 55 |
| 80 | 512 | 55 |
| 90 | 523 | 60 |
| 100 | 548 | 60 |
| 110 | 564 | 65 |
| 120 | 600 | 60 |

Run: CFC 5-10-2 $\omega^2 t = 178 \times 10^7$ rad.$^2$/sec.

Sample Range: Fraction 10-130 $\omega^2 t \times (\rho_p - \rho_0) = 6.12$

| Fraction Number | $D_m$ (nm.) ± 5 nm. | $\sigma$ (nm.) ± 5 nm. |
|---|---|---|
| 20 | 414 | 20 |
| 30 | 435 | 35 |
| 40 | 492 | 40 |
| 50 | 523 | 40 |
| 60 | 543 | 50 |
| 70 | 580 | 50 |
| 80 | 611 | 50 |
| 90 | 626 | 45 |
| 100 | 647 | 50 |

Run: CFC 3-10-1 $\omega^2 t = 152 \times 10^7$ rad.$^2$/sec.

Sample Range: Fraction 5-125 $\omega^2 t \times (\rho_p - \rho_o) = 6.43$

| Fraction Number | $D_m$ (nm.) ± 10 nm. | $\sigma$ (nm.) ± 10 nm. |
|---|---|---|
| 20 | 414 | 30 |
| 30 | 414 | 35 |
| 40 | 435 | 50 |
| 50 | 486 | 50 |
| 60 | 517 | 50 |
| 70 | 543 | 50 |
| 80 | 574 | 55 |
| 90 | 605 | 55 |

Run: CFC 3-10-2 $\omega^2 t = 135 \times 10^7$ rad.$^2$/sec.

Sample Range: Fraction 5-115 $\omega^2 t \times (\rho_p - \rho_o) = 5.71$

| Fraction Number | $D_m$ (nm.) ± 5 nm. | $\sigma$ (nm.) ± 5 nm. |
|---|---|---|
| 20 | 409 | 25 |
| 30 | 435 | 40 |
| 40 | 486 | 45 |
| 50 | 523 | 40 |
| 60 | 543 | 45 |
| 70 | 580 | 50 |
| 80 | 611 | 45 |
| 90 | 621 | 55 |

conditions to test the reproducibility of the experiment. The fraction analyzed from the separation was taken from the peak of the absorbance versus fraction number output from the spectrophotometer. The results are listed in Table 6.

The results in Table 6 indicate that the rotor can be effectively calibrated to yield an average particle size. By modifying experimental conditions the range of particle size can be adjusted to fit the sample. This is of particular importance in the size range below 200 nm., where there are at present no accurate techniques of analysis. The scattering pattern for particles in this size range has no character (i.e., maxima and minima), therefore, is very insensitive to changes in $D_m$ and $\sigma$ .

Single Latex System

The single sample experiment was performed to test the limitations of the separation technique. Dow PS latex 1053-14-6 ($D_m$ 564 nm., $\sigma$ = 40 nm.) was used as the sample. A 5.0-10.0% sucrose gradient using the center unloading method was tested first. The output from the spectrophotometer showed a bimodal character, the first peak of a greater intensity than the second. The particle size increased logically until an analysis from the second peak was made. The fractions from the second peak were of a slightly smaller size with a wider distribution. A frequency versus diameter plot was generated from fractions of a run with an 8.0-10.0% sucrose gradient, run SFC 8-10-2, to better visualize the data. The fraction from the second peak has a greater proportion of smaller and larger particles than the first peak fraction. Since the fraction from the

TABLE 5

| (X) Fraction Number | (Y) $D_m$ (nm.) Observed | $D_m$ (nm.) Theoretical |
|---|---|---|
| 20 | 409 | 415 |
| 30 | 435 | 447 |
| 40 | 486 | 478 |
| 50 | 523 | 510 |
| 60 | 543 | 541 |
| 70 | 580 | 573 |
| 80 | 611 | 605 |
| 90 | 621 | 637 |

Experimental and Theoretical Diameters Obtained from Least Squares Fit of Particle Size vs. Fraction Number Plot of Run CFC 3-10-2

TABLE 6

| Sample | $D_m$ (nm.) Initial ± 5 nm. | $D_m$ (nm.) Theoretical ± 10 nm. |
|---|---|---|
| 1053-14-2 | 435 | 447 |
| 1053-14-4 | 502 | 510 |
| 1053-14-7 | 585 | 605 |

Comparison of Experimental and Theoretical Diameters to Test the Reproducibility of the Separation Experiment

Figure 4. Plot of Frequency vs. Diameter of Fractions Under Peaks from Run SFC 8-10-2

Fig. 4

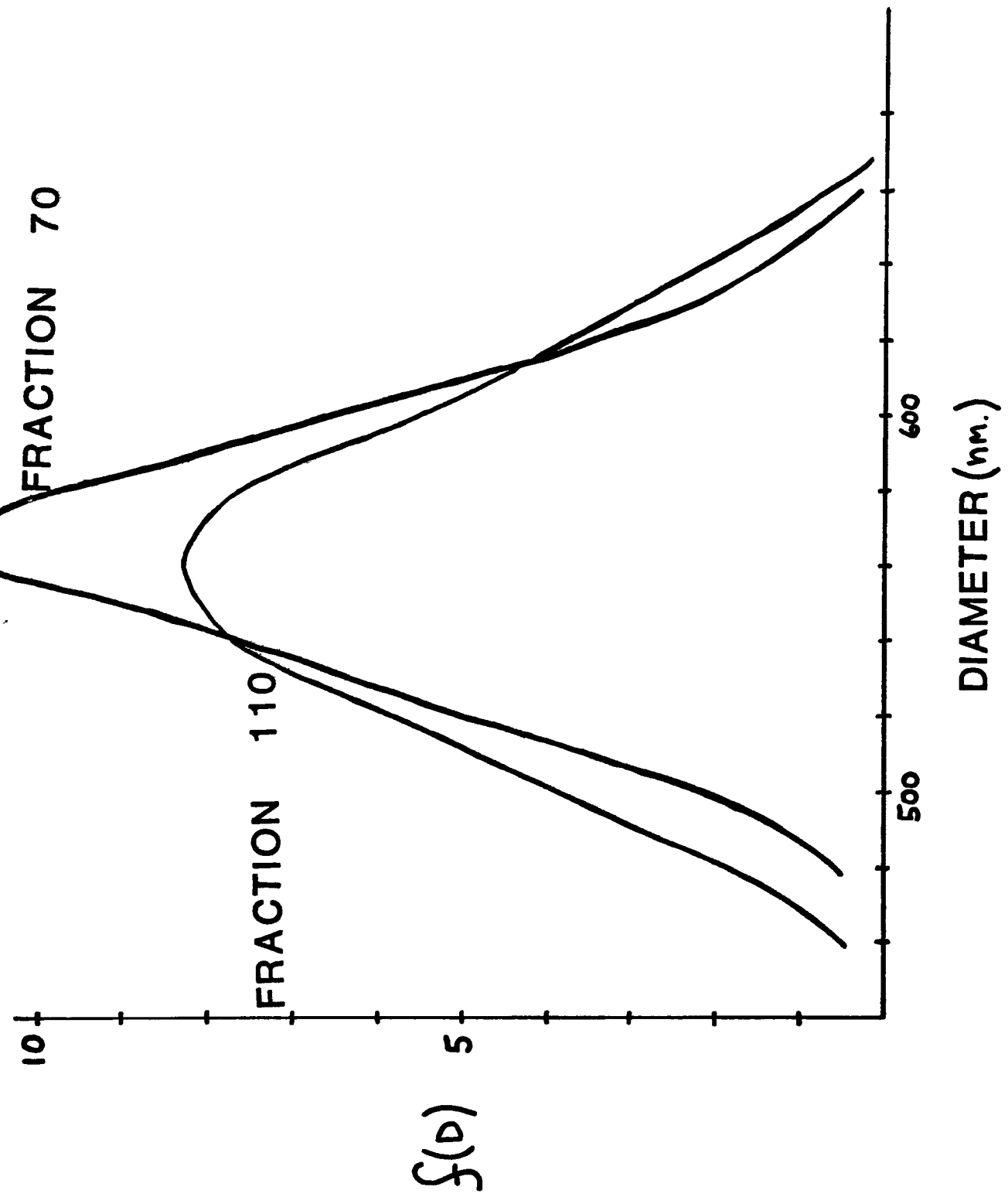

second peak was in the rotor for a longer period of time, the smaller particles had begun to catch up with the larger ones resulting in the wider size distribution and smaller size. The separation of the two peaks indicates that a continuous monomodal system was not present. A second run was made with the 5.0-10.0% gradient, this time with a lower $\omega^2 t$ value. The same bimodal character was exhibited from the spectrophotometer and light scattering analysis gave similar results. Still employing the center pump-out method, an 8.0-10.0% gradient was run. The standard deviation values were lower and the bimodal character again appeared. This run was repeated with a slightly greater $\omega^2 t$ value and the same results obtained.

The next series of experiments involved the edge-unloading method with an 8.0-10.0% sucrose gradient. This method gave, for the first run, lower $\sigma$ values and a mirror image of the bimodal distribution obtained from the center-unloading method. (i.e., the first peak had a lower intensity than the second). This indicates that the two peaks are the result of the sample and not the separation technique, and further strengthens the existence of a bimodal distribution. The diagram on the following page illustrates the difference between the two techniques. The runs are SFC 8-10-2 and SFE 8-10-2 which have approximately the same $\omega^2 t$ value. A second run was made with the 8.0-10.0% gradient this time with a lower $\omega^2 t$ value. The resulting $\sigma$ values were the lowest and most consistent of all the runs.

Figure 5. Spectrophotometer Output of Runs SFC 8-10-2 and SFE 8-10-2

Fig. 5

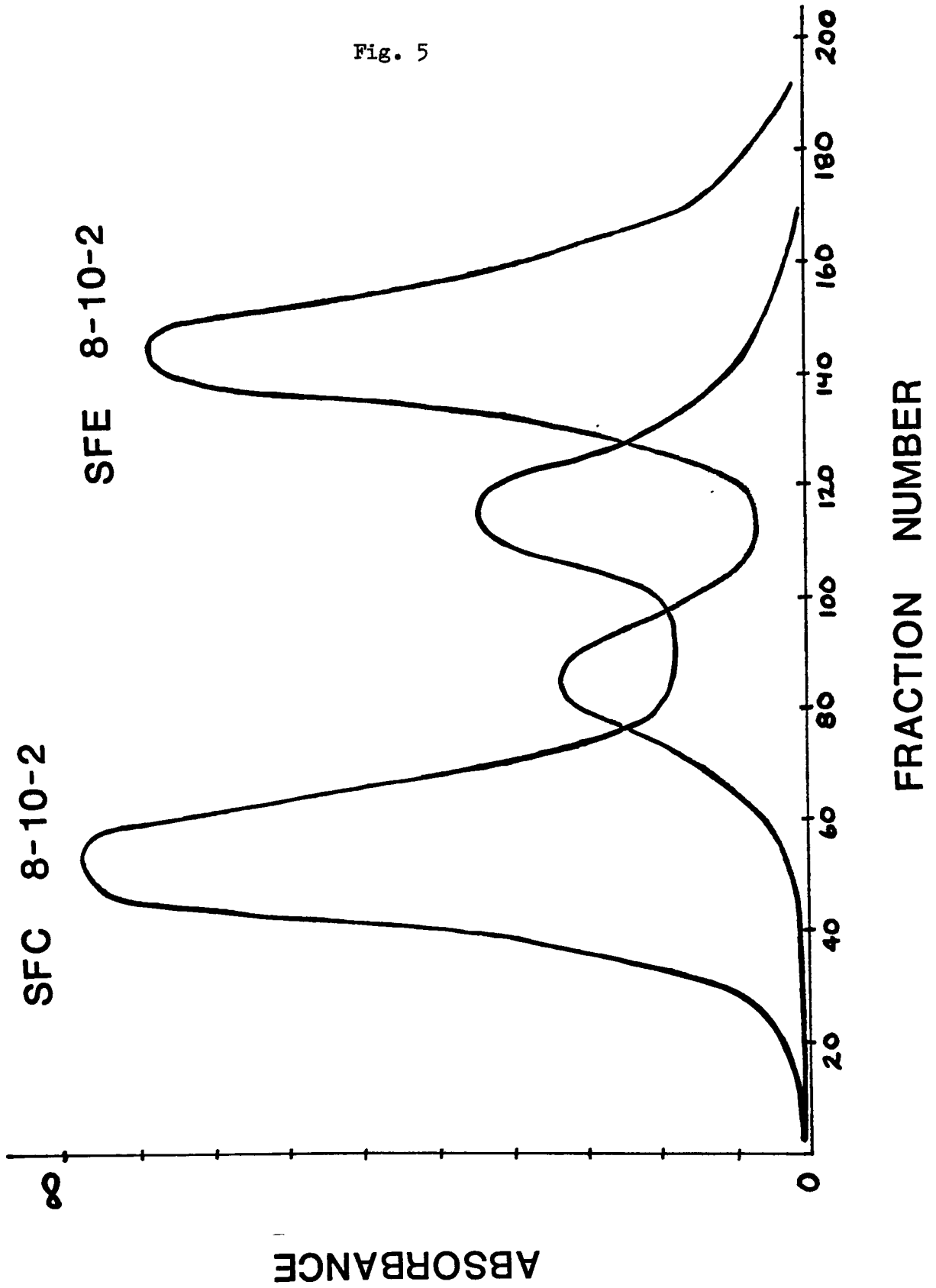
SFC 8-10-2
SFE 8-10-2
ABSORBANCE
FRACTION NUMBER
0
∞
20
40
60
80
100
120
140
160
180
200

TABLE 7

Light Scattering Results of Fractions from Separation Runs On Polystyrene Latex 1053-14-6.

Run: SFC 5-10-1 $\omega^2 t = 182 \times 10^7$ rad.$^2$/sec.

| Fraction Number | $D_m$ (nm.) ± 5 nm. | $\sigma$ (nm.) ± 5 nm. |
|---|---|---|
| 40 | 548 | 40 |
| 50 | 559 | 30 |
| 60 | 559 | 30 |
| 70 | 559 | 40 |
| 80 | 559 | 30 |
| 100 | 564 | 25 |
| 140 | 559 | 40 |

Run: SFC 5-10-2 $\omega^2 t = 163 \times 10^7$ rad.$^2$/sec.

| Fraction Number | $D_m$ (nm.) ± 5 nm. | $\sigma$ (nm.) ± 5 nm. |
|---|---|---|
| 20 | 559 | 30 |
| 30 | 559 | 35 |
| 80 | 564 | 50 |
| 120 | 559 | 40 |

Run: SFC 8-10-1 $\omega^2 t = 244 \times 10^7$ rad.$^2$/sec.

| Fraction Number | $D_m$ (nm.) ± 5 nm. | $\sigma$ (nm.) ± 5 nm. |
|---|---|---|
| 15 | 554 | 30 |
| 20 | 559 | 30 |
| 30 | 559 | 30 |
| 40 | 559 | 30 |

Run: SFC 8-10-2 $\omega^2 t = 259 \times 10^7$ rad.$^2$/sec.

| Fraction Number | $D_m$ (nm.) ± 5 nm. | $\sigma$ (nm.) ± 5 nm. |
|---|---|---|
| 40 | 554 | 35 |
| 50 | 559 | 30 |
| 60 | 564 | 30 |
| 70 | 559 | 35 |
| 110 | 554 | 45 |

Run: SFE 8-10-1 $\omega^2 t = 288 \times 10^7$ rad.$^2$/sec.

| Fraction Number | $D_m$ (nm.) ± 5 nm. | $\sigma$ (nm.) ± 5 nm. |
|---|---|---|
| 20 | 564 | 40 |
| 90 | 564 | 30 |
| 120 | 559 | 30 |
| 140 | 559 | 35 |

Run: SFE 8-10-2 $\omega^2 t = 250 \times 10^7$ rad.$^2$/sec.

| Fraction Number | $D_m$ (nm.) ± 5 nm. | $\sigma$ (nm.) ± 5 nm. |
|---|---|---|
| 130 | 564 | 30 |
| 135 | 569 | 25 |
| 140 | 569 | 25 |
| 150 | 564 | 30 |

The next step in the investigation would be to take fractions with lower $\sigma$ values and attempt a further fractionation. Adjacent fractions were mixed so that the resulting fractions would be of a sufficient concentration to be analyzed. An 8.0-10.0% gradient was used with the center-unloading method. The output from the spectrophotometer showed just one peak, again further support of a bimodal distribution of the original sample. The standard deviation values were lowered from 30 to 25. Another run was performed on fractions which had $\sigma$ values of 25, this time with the edge unloading method. The resulting fractions had higher $\sigma$ values.

TABLE 8

Light Scattering Results from Refractionation of Polystyrene Latex 1053-14-6

Run: SRC 8-10-1 $\omega^2 t = 244 \times 10^7$ rad.$^2$/sec.

| Fraction Number | $D_m$ (nm.) ± 5 nm. | $\sigma$ (nm.) ± 5 nm. |
|---|---|---|
| 20 | 554 | 35 |
| 30 | 559 | 25 |
| 40 | 564 | 25 |
| 50 | 564 | 25 |

Run: SRE 8-10-1 $\omega^2 t = 271 \times 10^7$ rad.$^2$/sec.

| Fraction Number | $D_m$ (nm.) ± 5 nm. | $\sigma$ (nm.) ± 5 nm. |
|---|---|---|
| 140 | 559 | 40 |
| 145 | 554 | 40 |
| 150 | 554 | 45 |
| 160 | 554 | 40 |

It appears that a standard deviation value of 25 nm. is the lower limit of this sample. This means that 95% of the size distribution lies within a range of ± 25 nm.

The ultimate efficiency of separation can be calculated and compared to the experimental result. A particle size of 500 nm., a distance of 5.0 cm. from the center of the rotor, and a volume element of 10 cubic centimeters is assumed in the calculation below:

$$V = \pi r^2 h$$

$$\frac{dV}{dr} = 2\pi r h$$

$$dr = \frac{dV}{2\pi r h}$$

The height of the rotor is 7.5 cm. and substituting into the equation yields

$$dr = \frac{10\ cm^3}{2 \times \pi \times 5.0\ cm \times 7.5\ cm} = 4.2 \times 10^{-2}\ cm$$

From the results of the rotor calibration a plot of particle size (D) versus rotor radius can be generated.

TABLE 9

Calibration Data - Diameter vs. Rotor Distance

| Diameter (cm. x $10^6$) | Radial Distance (cm.) |
|---|---|
| 415 | 3.586 |
| 447 | 4.096 |
| 478 | 4.539 |
| 510 | 4.936 |
| 541 | 5.300 |
| 573 | 5.637 |
| 605 | 5.935 |
| 637 | 6.251 |

A least squares analysis was performed on the data and a slope $\left(\frac{dD}{dr}\right)$ obtained. The value from above is $11.8 \times 10^{-5}$ cm/cm and when multiplied by $dr$ gives a $dD$ value for a fraction at that location in the rotor. That is the range of diameters in the element .

$$\frac{dD}{dr} \times dr = 11.8 \times 10^{-5} \frac{cm}{cm} \times 4.2 \times 10^{-2} cm. = 5.0 \times 10^{-6} cm$$

This is equivalent to 5.0 nm. per fraction if all the particles were perfectly ordered in the rotor with no mixing. The difference can be attributed largely to the manner in which the particles leave the rotor. In either pump-out method the particles exit through four channels. This disturbs whatever order the particles have achieved in the rotor and consequently broadens the size distribution of the fractions.

Chemically Mixed Latex System

The first chemically mixed system consisted of Dow PS 1053-14-1, Monsanto PVC 540876, and Kodak PVA latex. In order to prevent coagulation no sucrose was added to the sample and the latex concentration was lowered from that of the previous systems. The output from the spectrophotometer showed three distinct peaks. A scattering pattern was obtained for a fraction from each area, and then compared to the original patterns of the latexes for peak assignments.

TABLE 10

Size Distribution Parameters of Latexes Before and After Separation Run

| Latex System | Analysis Before Mixing | | Analysis of Fractions | |
|---|---|---|---|---|
| | $D_m$(nm.) ± 5nm. | $\sigma$ (nm.) ± 5nm. | $D_m$(nm.) ± 5nm. | $\sigma$ (nm.) ± 10nm |
| PS | 409 | 20 | 404 | 25 |
| PVC | 419 | 20 | 424 | 30 |
| PVA | 228 | 30 | 238 | 25 |

Studies[10] have been performed on latex systems with added "impurities" to observe the effect on the scattering pattern. As an example latex of size $D_m$ = 240 nm. was combined with a 0.1% by number latex of $D_m$ = 1100 nm. The scattering pattern resulting from the mixture was very different from that of the separate samples. From the almost superimposable agreement of the scattering patterns it appears that a clean separation was achieved. However, the scattering pattern ($\rho$ vs $\theta$) for PVC and PS are similar due to the fact that both samples have similar $D_m$, $\sigma$ values. Therefore, another system was used to

illustrate a clean separation. This second mix consisted of Dow PS 1053-14-7, Monsanto PVC 540876, and Kodak PVA latex. The same experimental conditions were applied to this run as the last. The output from the spectrophotometer again recorded three distinct peaks and fractions from each area were analyzed.

TABLE 11

Size Distribution Parameters of Latexes Before and After Separation Run

| Latex System | Analysis Before Mixing | | Analysis of Fractions | |
|---|---|---|---|---|
| | $D_m$(nm.) ± 5 nm. | $\sigma$(nm.) ± 5 nm. | $D_m$(nm.) ± 5 nm. | $\sigma$(nm.) ±10nm. |
| PS | 585 | 40 | 580 | 45 |
| PVC | 419 | 25 | 424 | 30 |
| PVA | 228 | 30 | 235 | 30 |

Again the scattering patterns were "superimposable" indicating a clean separation.

Other attempts were made to analyze the fractions for chemical composition. An extraction into an organic layer followed by an infra-red analysis was inconclusive. The fractions were freeze dried to coagulate the latex then washed to remove the sucrose, however, this also was not successful. The prohibitively low concentration of latex in the fractions coupled with the sucrose media made these attempts of identification impractical.

Our development of a combined light scattering-ultracentrifugation technique to determine the size distribution parameters of polymer latex systems, can now be applied to broad continuous distributions, where a particle size calibration of the rotor can be achieved. To a monomodal distribution to obtain a more "monodisperse" sample that can be characterized more easily. Lastly, to mixtures of chemically different latex systems which can be cleanly separated by the centrifugation technique.

Figure 6. Spectrophotometer Output of First Separation Run on PS, PVC, PVA Mixture.

Fig. 6

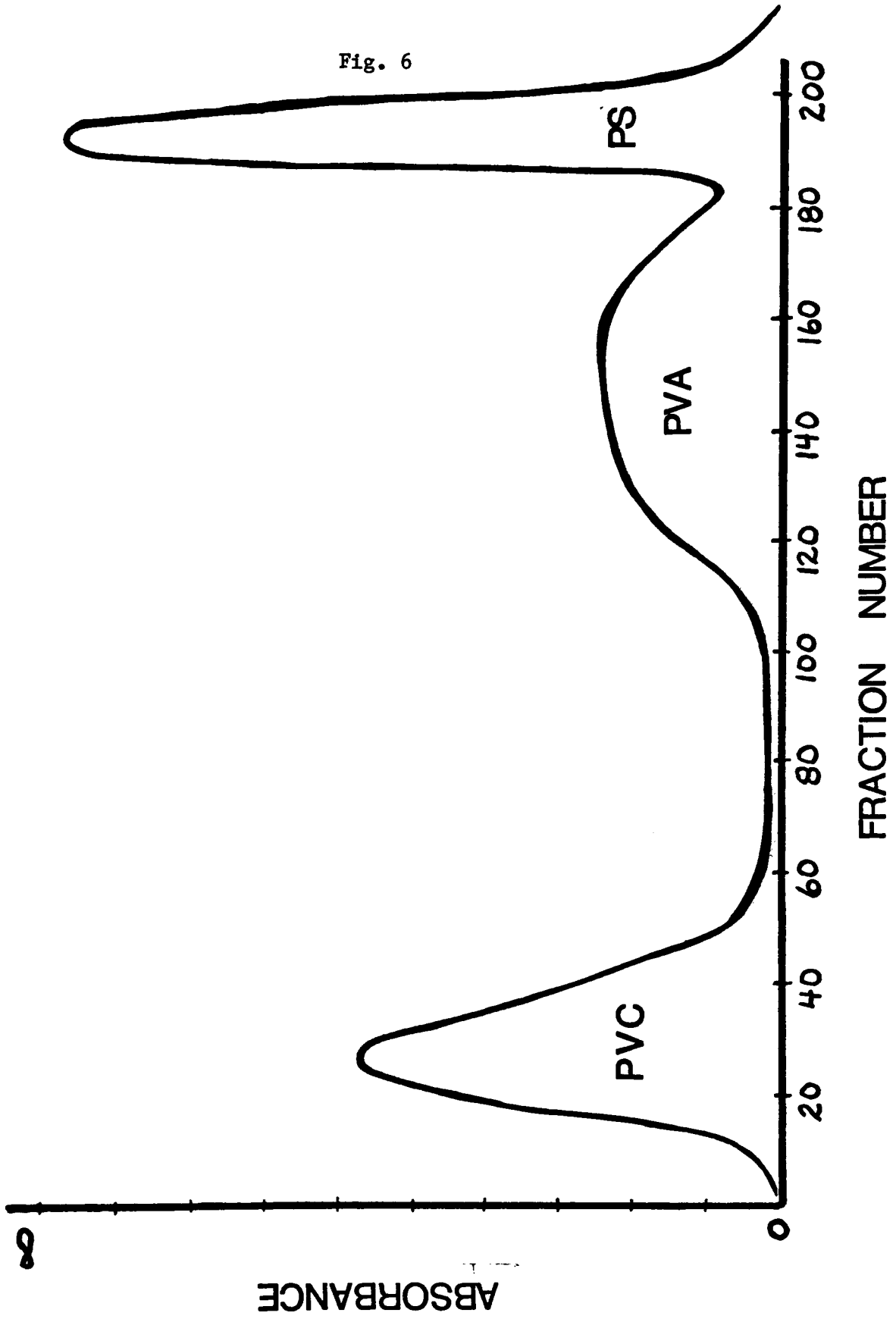
ABSORBANCE
0
20
40
60
80
100
120
140
160
180
200
FRACTION NUMBER
PVC
PVA
PS

Figure 7. Scattering Pattern of PVC Latex and Fraction 30 From First Separation Run

Fig. 7

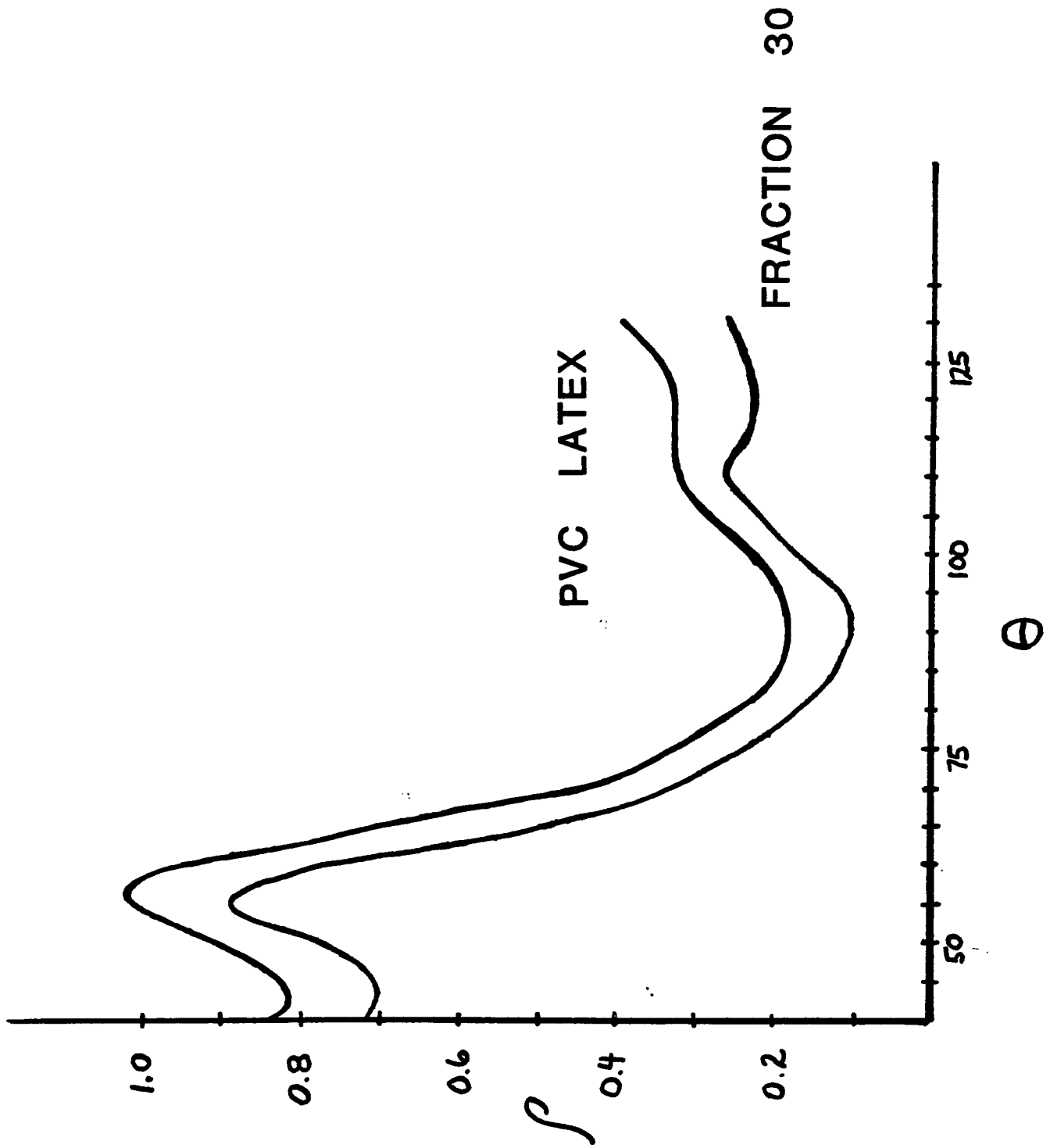

Figure 8. Scattering Pattern of PVA Latex and Fraction 150 from First Separation Run

Fig. 8

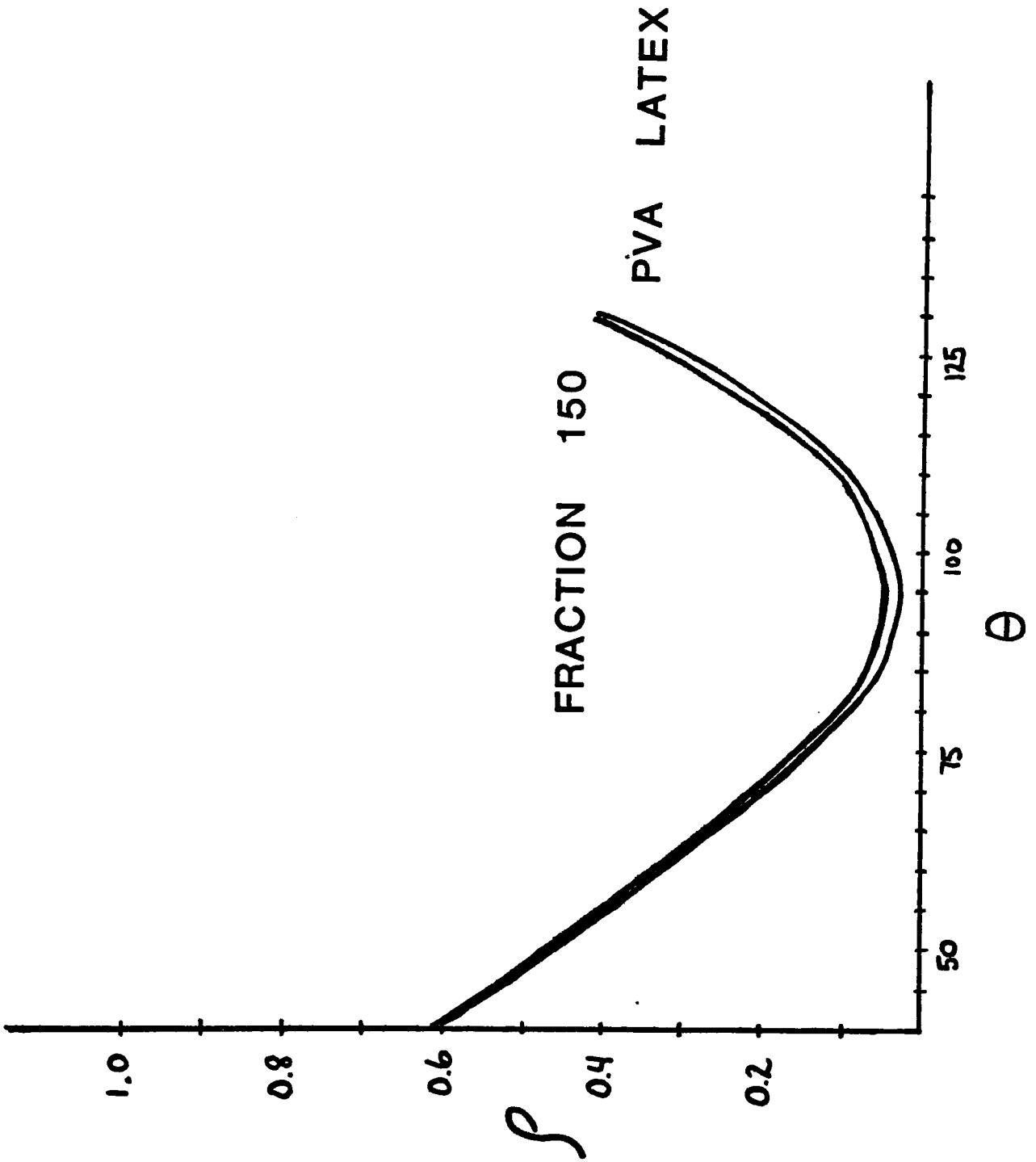

Figure 9. Scattering Pattern of PS Latex and Fraction 190 from First Separation Run

Fig. 9

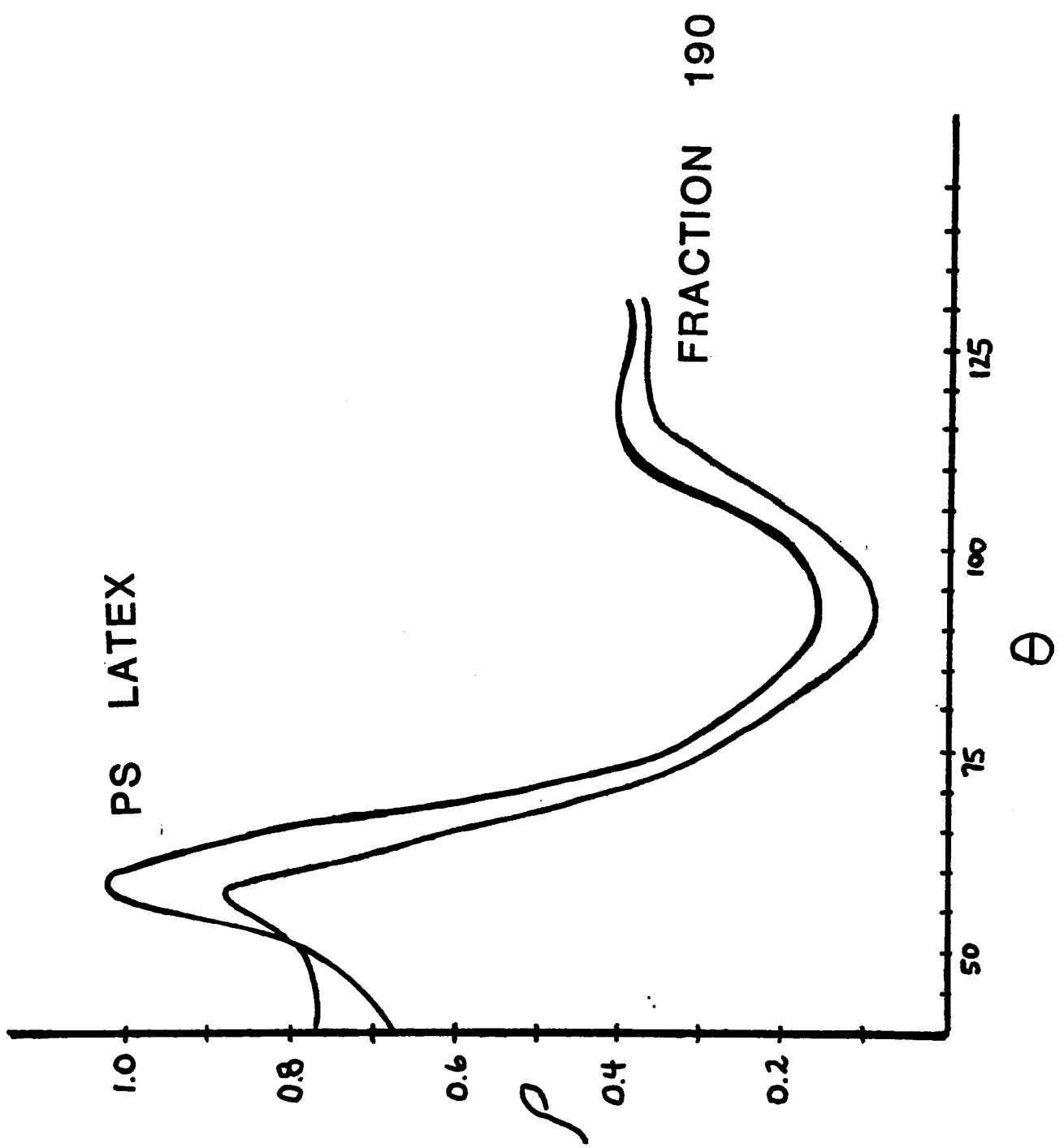

## REFERENCES


1. K. Linderstrom-Lang, Nature, 139, 713 (1937).

2. M. Behrens, Abt. 5, Teil 10, pt. 2, p. 1363, Urban und Scharzenberg, Berlin (1938).

3. M.K. Brakke, J. Am. Chem. Soc., 73, 1847 (1951).

4. N.G. Anderson, Nat. Cancer Inst. Mono. 21, 1 (1966).

5. T.P. Wallace, J. Poly. Sci., Part A, 9, 595 (1971).

6. M. Kerker, The Scattering of Light and Other Electromagnetic Radiation, Academic Press, New York, 1969.

7. W.F. Espenschied, M. Kerker, and E. Matijevic, J. Phy. Chem. 68, 3093 (1964).

8. J. Kratohvil, Clarkson College of Technology.

9. J. Gregory, J. of Colloid and Interface Sci., 42, 448 (1973).

10. T.P. Wallace, Ph.D. Thesis, Clarkson College of Technology, Potsdam, N.Y., 1967.